Ku-Band Phase-Gradient Metasurface for Broadband High-Gain Circularly Polarized Lens Antenna

Jianxun Su [1], Zhi Li [1], Zengrui Li [1], Qingxin Guo [1], and Yaoqing (Lamar) Yang [2]

[1] School of Information Engineering
Communication University of China, Beijing, 100024, China
zrli@cuc.edu.cn

[2] Department of Electrical and Computer Engineering
University of Nebraska-Lincoln, Nebraska, 68182, USA

Abstract ─ In this paper, a novel broadband high-gain, circularly polarized planar lens antenna is presented. We used the rotation elements to design a transmission-type polarization conversion planar phase-gradient metasurface (PPGM). By adjusting the rotational angles of the metal patch on the element, we obtained the desired transmission phase shift for PPGM. We used a patch antenna as a feed source, which formed a lens antenna system integrated with the PPGM. The simulation results showed that the PPGM can achieve a high-efficiency, cross-polarization conversion for vertical incidence of a right-handed circularly polarized plane wave. Our numerical and experimental results agreed well with each other, indicating that the antenna system had a peak gain of 18.8 dB, a good axial ratio better than 2 dB at 13 GHz, with an aperture efficiency of 50.56% and a focal length/diameter (F/D) ratio of 0.307. In addition, its -10 dB impedance and 3dB axial ratio bandwidth reached up to 940 MHz. The lens antenna performed well and can be applied in many communication systems.

Index Terms─ Circular polarization, lens antenna, planar phase-gradient metasurface (PPGM), plane wave.

I. INTRODUCTION

In recent years, metasurfaces have been attracting more research due to their remarkable ability to manipulate the reflections or transmissions of incoming waves in communication systems. A metasurface (MS) is the two-dimensional plane of metamaterials. Their extraordinary flexibility enables the amplitude, phase, and polarization of electromagnetic waves to be tailored. Metasurfaces have been widely used in stealth technology, high performance antennas, polarization modulation, and other applications [1].

As a pioneer in MS research, the Capasso group has realized a planar phase-gradient metasurface (PPGM) in the optical band through the "V" structure [2] for the first time and has verified the singular refraction which satisfies the generalized Snell's law of refraction. The PPGM has a greater degree of freedom in the direction of propagation of the wave emitted, which can change the beam propagation direction by the phase accumulation of propagation paths. The PPGM's subwavelength thickness structure can contribute greatly to the miniaturization of optical components. So far, there are usually three ways of implementing phase regulation. The first approach is to change the size of the structure. For example, Li et al. [3], who has designed the reflective focusing metasurface to achieve phase changes by varying the size of the H-shaped element. The second approach is to load active components. For example, Zhu et al. [4], uses the loading of active components to design an adjustable impedance metasurface to achieve a reflection wave which has a phase shift of 360 degrees. The third approach is to implement phase control of a circularly polarized wave by using a rotating unit and the Pancharatnam-Berry phase principle. For example, Yu et al. [5], designed a circularly polarized reflectarray antenna that uses a rotating, single-layer, fractured square ring. Motivated by such achievements, we designed a single-layer rotating element to build a focusing MS and a high-gain broadband, circularly polarized lens antenna.

At present, the most used method of transmission of a PPGM changes the unit structure size and multilayer structure to achieve an efficient goal [6]. Those methods have inherent challenges, such as complex processing, high cost, and difficult integration. This paper presented a single-layer, high-efficiency transmission PPGM designed using the element rotation technique, which effectively overcomes these shortcomings. First, we designed a single-layer, double E-shaped metasurface element, as shown in Fig. 1 (a). When the circularly polarized wave is vertically incident in the 12-14 GHz band, the transmitted wave is efficiently converted into a cross-polarized wave resulting in singular refraction.

Then, we took advantage of the principle that the rotation unit can control the phase of the circularly

Submitted On: May 22, 2018
Accepted On: December 29, 2018

polarized wave and designed a broadband, two-dimensional, transmission-type polarization conversion focusing planar phase-gradient metasurface [7,8]. Furthermore, a circularly polarized patch antenna was placed at the focal point as the feed source, and the near-plane wave was transmitted to the focusing PPGM, which greatly improves the gain of the feed. Thus, a low-profile broadband, circularly polarized, high-gain planar lens antenna can be realized in the Ku-band.

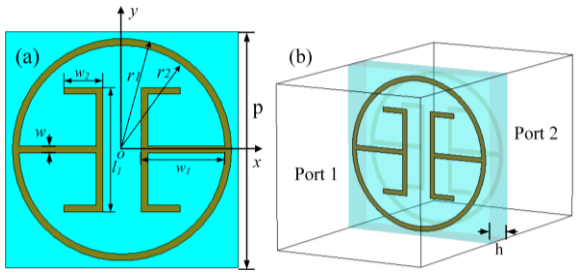

Fig. 1. Configuration of the proposed metasurface unit cell and the simulated setup: (a) top view and (b) perspective view.

II. ANALYSIS AND DESIGN

A. Design of the PPGM unit cell

To convert the circularly polarized spherical wave emitted from a feed source into a cross-polarized plane wave, we first utilized the element rotation method [9] to compensate for the phase deviation of a circularly polarized wave. Then we designed a unit cell to realize polarization conversion of a circularly polarized wave. According to the Pancharatnam-Berry phase principle, when the x-polarized wave and the y-polarized wave illuminate the unit, respectively, it must satisfy two critical requirements: first, the transmissive phase difference of the x-polarized (ϕ_x) and y-polarized (ϕ_y) wave should meet with $|\phi_x - \phi_y| = \pi$ to ensure a pure circularly polarized transmission wave, and second, the amplitudes of the transmission coefficient of the x-polarized (T_x) and y-polarized (T_y) wave should be equal and as close to 1 as possible to improve the transmission efficiency.

The transmission process of circularly polarized waves is deduced as follows. Assume that a right-handed circularly polarized (RHCP) wave is vertically incident onto a unit cell along the +z direction, as shown in Fig. 1 (a). The E field of the incident RHCP wave can be expressed as:

$$\boldsymbol{E}_i = (\hat{\boldsymbol{x}} - j\hat{\boldsymbol{y}})e^{-jkz}, \tag{1}$$

and the transmitted wave is:

$$\boldsymbol{E}_t = (\hat{\boldsymbol{x}}T_x e^{j\phi_x} - j\hat{\boldsymbol{y}}T_y e^{j\phi_y})e^{-jkz}, \tag{2}$$

where T_x and T_y are the amplitudes of the transmission coefficient of the x-polarized and y-polarized wave components, and ϕ_x and ϕ_y are the phase shifts of the x-polarized and y-polarized components of the incident wave. When the metallic unit structure is rotated by θ, as shown in Fig. 2 (a), the rotated coordinate can be written as:

$$\begin{cases} \hat{\boldsymbol{x}} = \hat{\boldsymbol{x}}'\cos\theta - \hat{\boldsymbol{y}}'\sin\theta, \\ \hat{\boldsymbol{y}} = \hat{\boldsymbol{x}}'\sin\theta + \hat{\boldsymbol{y}}'\cos\theta, \end{cases} \tag{3}$$

and the incident wave in the rotated coordinate is expressed as:

$$\begin{aligned} \boldsymbol{E}_i &= [(\hat{\boldsymbol{x}}'\cos\theta - \hat{\boldsymbol{y}}'\sin\theta) - j(\hat{\boldsymbol{x}}'\sin\theta + \hat{\boldsymbol{y}}'\cos\theta)]e^{-jkz} \\ &= (\hat{\boldsymbol{x}}' - j\hat{\boldsymbol{y}}')e^{-jkz}e^{-j\theta}. \end{aligned} \tag{4}$$

Then, the transmitted wave is:

$$\boldsymbol{E}_t = (\hat{\boldsymbol{x}}'T_x'e^{j\phi_x'} - j\hat{\boldsymbol{y}}'T_y'e^{j\phi_y'})e^{-jkz}e^{-j\theta}. \tag{5}$$

In the xyz coordinate, as $\phi_x = \phi_x'$ and $\phi_y = \phi_y'$, $T_x = T_x'$, and $T_y = T_y'$, the transmitted wave can be written as:

$$\begin{aligned} \boldsymbol{E}_t &= [(\hat{\boldsymbol{x}}\cos\theta + \hat{\boldsymbol{y}}\sin\theta)T_x e^{j\phi_x} - j(-\hat{\boldsymbol{x}}\sin\theta + \hat{\boldsymbol{y}}\cos\theta)T_y e^{j\phi_y}]e^{-jkz}e^{-j\theta} \\ &= \frac{1}{2}(\hat{\boldsymbol{x}} + j\hat{\boldsymbol{y}})(T_x e^{j\phi_x} - T_y e^{j\phi_y})e^{-jkz}e^{-j2\theta} \\ &\quad + \frac{1}{2}(\hat{\boldsymbol{x}} - j\hat{\boldsymbol{y}})(T_x e^{j\phi_x} + T_y e^{j\phi_y})e^{-jkz} \end{aligned}. \tag{6}$$

From (6), the transmitted wave consists of two parts: the left-hand rotation $\boldsymbol{E}_{t(\mathrm{LHCP})}$ and right-hand rotation $\boldsymbol{E}_{t(\mathrm{RHCP})}$ components. When $T_x = T_y = T$ and $|\phi_x - \phi_y| = \pi$, the following result can be obtained using equation (6):

$$\begin{aligned} \boldsymbol{E}_{t(LHCP)} &= \frac{T}{2}(\hat{\boldsymbol{x}} + j\hat{\boldsymbol{y}})(1 - e^{j(\pm\pi)})e^{j\phi_x}e^{-jkz}e^{-j2\theta} \\ &= T(\hat{\boldsymbol{x}} + j\hat{\boldsymbol{y}})e^{j\phi_x}e^{-jkz}e^{-j2\theta} \end{aligned}, \tag{7}$$

$$\begin{aligned} \boldsymbol{E}_{t(RHCP)} &= \frac{T}{2}(\hat{\boldsymbol{x}} - j\hat{\boldsymbol{y}})(1 + e^{j(\pm\pi)})e^{j\phi_x}e^{-jkz} \\ &= 0 \end{aligned}. \tag{8}$$

From (7) and (8), we can see that after the right-handed circularly polarized wave is transmitted through the unit cell, it is converted into a left-handed circularly polarized wave [10]. The transmission phase of the transmitted wave, with respect to the incident wave, is doubled.

The unit cell of the PPGM designed is shown in Fig. 2 (b). It is composed of two metallic layers and one intermediate dielectric layer with thickness of 1.5 mm, relative permittivity of 2.65 and loss tangent of 0.0026. The detailed parameters of the structure depicted in Fig. 1 are p=7mm, r_1=3.3mm, r_2=3.1mm, l_1=3.5mm, w=0.2 mm, w_1 = 2.218 mm, w_2 = 1.06 mm, and h = 1.5 mm. The unit cell was simulated with CST Microwave Studio® by using periodic boundary.

Figure 3 shows the phase and amplitude curves of the transmitted wave under x-polarized and y-polarized waves, respectively. It is shown that the amplitude T_x= T_y=0.94 and the phase $|\phi_x - \phi_y| = \pi$ at 13 GHz. Therefore, this unit cell can be used for efficient cross-polarization transmission under the condition of a circularly polarized incident wave. A RHCP plane wave illuminates on the unit cell vertically along the +z direction.

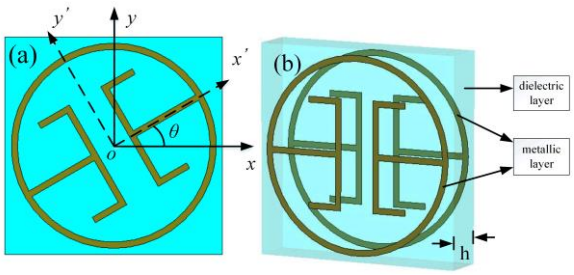

Fig. 2. (a) The rotation angle of the metallic unit, and (b) the composition of the metal unit.

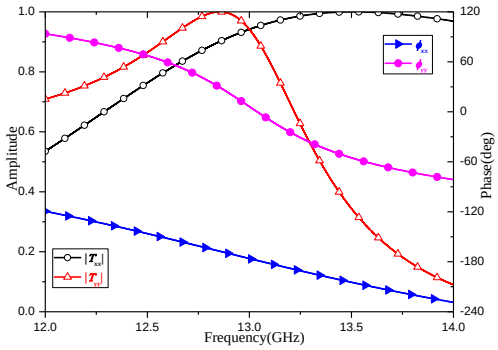

Fig. 3. Amplitude and phase of transmitted wave under x-polarized and y-polarized plane wave illumination.

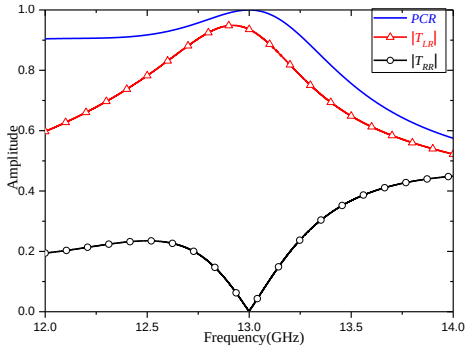

Fig. 4. The transmission amplitude and PCR under RHCP wave incidence.

Figure 4 shows that the cross-polarization transmission amplitude $|T_{LR}|$ reaches 0.94 at about 13 GHz. We used the polarization conversion ratio (PCR) to characterize the proportion of the cross-polarized component in the transmitted wave, and the PCR is defined as:

$$PCR = T_{LR}^2 / \left(T_{LR}^2 + T_{RR}^2\right), \tag{9}$$

where T_{LR} is the cross-polarization transmission coefficient and T_{RR} is the co-polarized transmission coefficient. From the PCR curve calculated by equation (9), we can see that the cross polarization conversion rate is greater than 90% in 12 ~13.3 GHz, which indicates that the RHCP plane wave is efficiently converted into a LHCP plane wave after transmitting the unit.

To verify the phase and polarization conversion characteristics of the rotating unit, we used the RHCP plane wave to illuminate the rotated elements respectively along the +z direction. In Fig. 5, the element is rotated with a step of 30°, and then we get the transmitted waves (LHCP) which achieves an accurate phase shift of 2θ. Meanwhile, these transmission amplitudes are almost equal and maintained up to 0.94. The above results demonstrate the high transmission and cross-polarization conversion characteristics of the unit cell, which meets the design requirements.

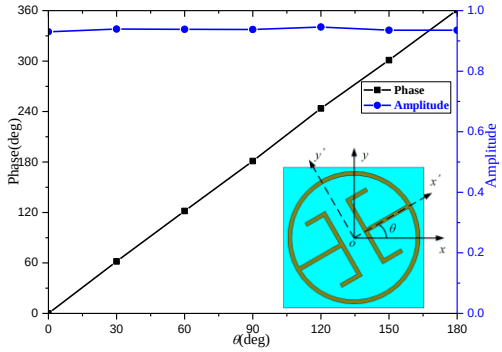

Fig. 5. The phase and amplitude of transmitted waves under RHCP plane wave illumination at 13 GHz.

B. Design of planar lens antenna based on PPGM

The unit can achieve efficient cross-polarization conversion over a wide frequency band and compensate for any phase offset in the range of [0, 2π] by the rotation unit. In order to enable the vertical incidence circularly polarized plane waves to converge to one point after transmitting the PPGM, the phase distribution of the elements in the xoy plane should be satisfied by the following parabolic equation:

$$\phi(x,y) = \frac{2\pi}{\lambda_0}\left(\frac{x^2+y^2}{4f}\right) + \phi_0 . \tag{10}$$

Where $\phi(x,y)$ is the required phase compensation at the point (x,y), ϕ_0 is the center point phase of the lens, λ_0 is the free space wavelength at the design frequency, and f is the physical focal distance from the center point of the feed source to the center point of the PPGM.

Due to the reversibility of the electromagnetic wave transmission [11], we placed a patch antenna on the focal point of the PPGM along the –z direction at xoy-plane that can radiate a right-handed circularly polarized wave at 13 GHz. The PPGM contained 11 × 11 structural units, and the optimal size of the overall PPGM was 79.2 × 79.2 mm^2. The focal length-to-diameter ratio (F/D) was 0.307. According to equation (10), the compensation phase of each unit can be calculated, and then the angle of rotation of each unit is obtained. The physical structure

diagram of the overall lens antenna system integrated with the PPGM is shown in Fig. 6.

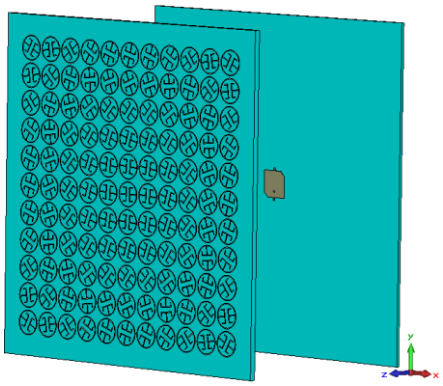

Fig. 6. The physical structure diagram of the overall lens antenna system integrated with the PPGM.

III. MEASUREMENT AND DISCUSSION

In Section II, we demonstrated our design of the overall PPGM lens antenna system at the Ku-band. Section III verified the radiation characteristics of the lens antenna by using CST software simulation with a transient solver. By fine-tuning the focal distance during simulation, we can obtained the optimal length of the focal distance (f = 28.5mm). Thus, we placed a feeding patch antenna 28.5 *mm* away from the PPGM along the −z-direction at xoy-plane. The E_x distributions of the patch antenna with and without the PPGM are shown in Fig. 7. As shown in Fig. 7, the PPGM lens transformed the quasi-sphere wave emitted from the patch antenna into a plane wave, as per the theoretical prediction. Due to the high directivity of the plane wave, the beam width of the patch antenna decreased greatly and the gain was remarkably enhanced.

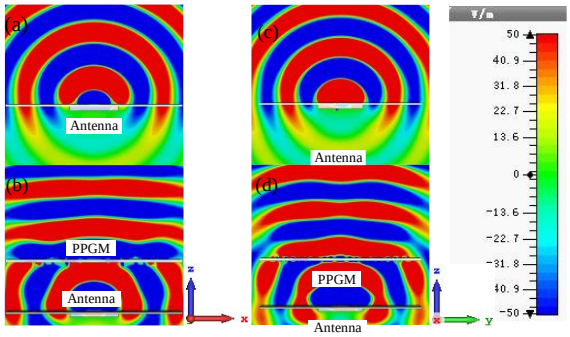

Fig. 7. Simulated electric field distributions (Ex) at 13 GHz. (a) xoz-plane for the patch antenna; (b) xoz-plane for the PPGM; (c) yoz-plane for the patch antenna; (d) yoz-plane for the PPGM.

Figure 8 depicts a three-dimensional (3D) simulation of the far-field radiation patterns of the patch antenna and the PPGM lens antenna at 13 GHz. It shows that the gain of the patch antenna was 7.68 dB, and the gain of the PPGM lens antenna was 18.8 dB. So we conclude that the PPGM lens can remarkably enhance the gain of the patch antenna at 13 GHz and that the peak gain of the patch antenna improved by 11.12 dB.

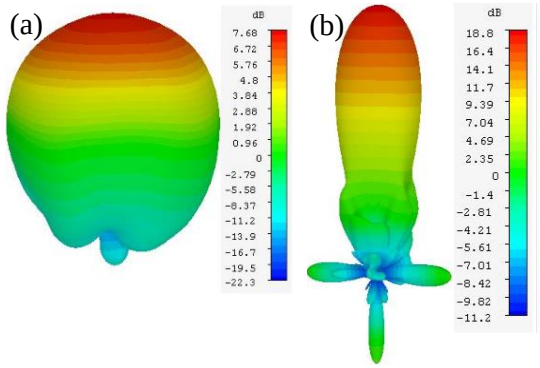

Fig. 8. The simulated 3D far-field radiation patterns at 13 GHz. (a) the patch antenna and (b) the PPGM lens antenna.

To validate the simulation results, the PPGM lens and patch antenna were fabricated, as shown in the photograph in Fig. 9 (a). The far-field measurement setup shown in Fig. 9 (b), the patch antenna was connected to the PPGM by four dielectric cylinders with a length of 28.5 mm.

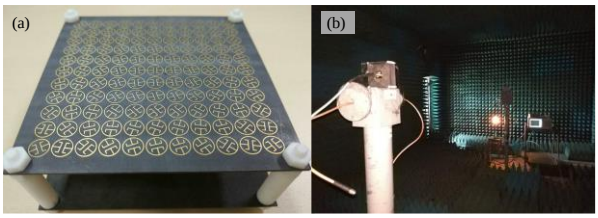

Fig. 9. Fabrication and measurement: (a) prototypes of the proposed PPGM lens antenna, and (b) measurement in anechoic chamber.

Figure 10 shows the structure of the patch antenna. It is a square metal radiation patch with a cutting angle, which is fed by a 50-Ω SMA connector on the bottom metallic layer. The substrate has a thickness of 0.787 mm, a relative permittivity of 2.2 and a loss tangent of 0.0009, and the size of the substrate was 79.2 × 79.2 mm^2. This feed patch antenna which can emit the RHCP wave, and when the wave illuminates the PPGM vertically, it will be converted into a LHCP wave. Figure 10 also shows the measured reflection coefficients of the patch antenna with and without the PPGM. It can be seen that the patch antenna with the PPGM operated at a broadband −10 dB bandwidth from 12.6 GHz to 13.54 GHz. Figure 11 shows the comparison of the simulated

and measured axial ratios of the patch antenna and the lens antenna. We found that the axial ratio was better than 2 dB around 13 GHz and operated at a broadband 3 dB axial ratio bandwidth ranging from 12.6 to 13.54 GHz. The simulated and measured radiation patterns in the xoz- and yoz-planes at 13 GHz are illustrated in Fig. 12. We observed that the PPGM lens enhanced the gain of the patch antenna considerably, and right-handed circularly polarized waves (RHCP) are well converted into left-handed circularly polarized waves (LHCP). Meanwhile, the half power beam width reduced from 81°to 16.5°. Figure 13 presents that the simulated and measured peak gains of the PPGM lens antenna versus frequency. We can see that the measured 1 dB gain bandwidth achieved by this PPGM lens antenna is 0.58 GHz (Fractional bandwidth of 4.5%). The measured gain is approximately 0.3 dB below the gain obtained in simulation. The discrepancy could be due to manufacturing tolerances or test environment tolerances. The overall measured and simulated results of the PPGM lens antenna are compared in Table 1. The measured results of the fabricated antenna were generally consistent with the simulation, which validates the proposed design methodology.

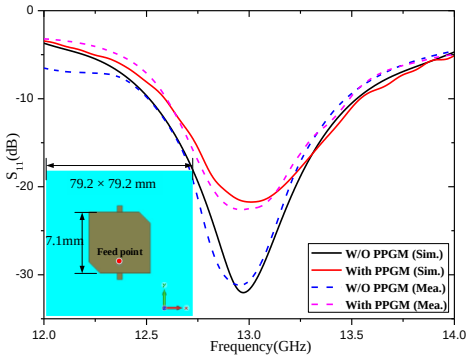

Fig. 10. Simulated and measured reflection coefficients of patch antenna with/without the PPGM.

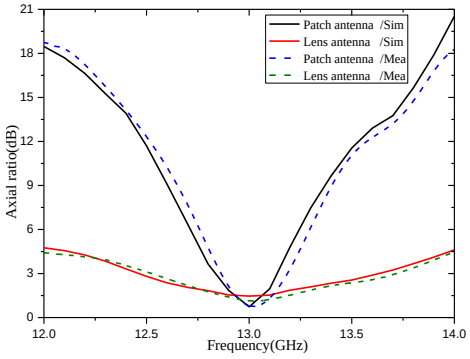

Fig. 11. Simulated and measured axial ratios of the patch antenna (RHCP) and the PPGM lens antenna (LHCP).

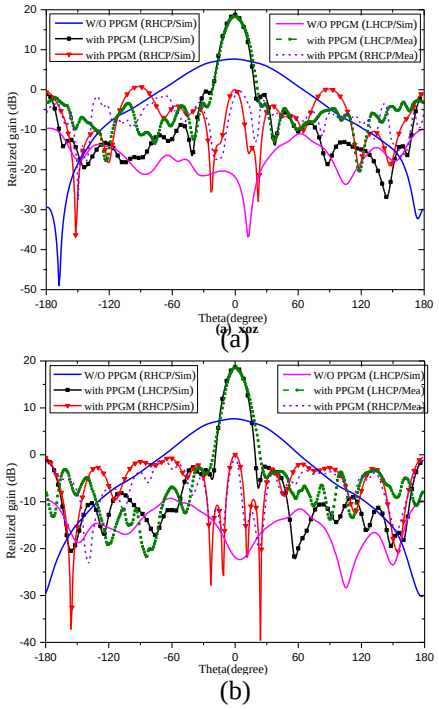

Fig. 12. Simulated and measured far-field radiation patterns of the patch antenna and the PPGM lens antenna at 13 GHz: (a) xoz-plane and (b) yoz-plane.

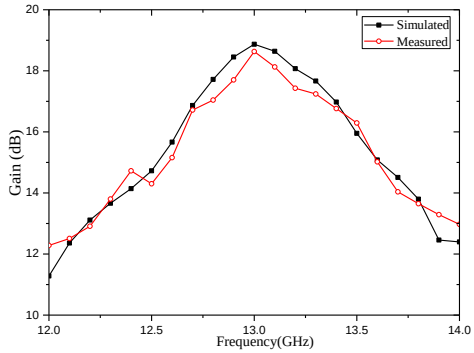

Fig. 13. Simulated and measured peak gains of the PPGM lens antenna versus frequency.

Table 1: Results comparison of measured and simulated PPGM lens antenna

Parameter	Measured Value	Simulated Value
Peak gain (dB)	18.5	18.8
1dB gain bandwidth	0.58GHz (4.5%)	0.67GHz (5.2%)
3 dB AR bandwidth	0.8GHz (6.15%)	0.94GHz (7.2%)
HPBW (degree)	16.5	17.2
Side lobe level (dB)	–18.2	-19.8

IV. CONCLUSION

In this paper, a new method of designing a high-gain broadband, circularly polarized planar lens antenna was proposed based on the element rotation method. The planar lens antenna was designed, fabricated, and measured at Ku-band. The PPGM had a thickness of 1.5 mm and dimensions of 79.2 × 79.2 mm^2 with an F/D of 0.307. High transmission and polarization conversion efficiency of the unit cell and great focusing effect of the PPGM guaranteed the good performance of the transmitting lens antenna, which achieved a peak gain of 18.8 dB, SLL of −18.2 dB, HPBW of 16.5°, F/B of 18.2 dB, axial ratio of 2 dB, and a high aperture efficiency of 50.56% at 13 GHz. This design provides a new approach for a low profile planar lens antenna with high gain, broadband, circularly polarized, high radiation efficiency. Thus, it can be widely used in long distance wireless communication and imaging sensing systems.

ACKNOWLEDGMENT

The authors are grateful to support from the National Natural Science Foundation of China under Grant No. 61331002, No. 61671415 and No. 61701448.

REFERENCES

[1] Y. F. Li, J. Q. Zhang, S. B. Qu, *et al*., "Wideband radar cross section reduction using two-dimensional phase gradient metasurfaces," *Appl. Phys. Lett.*, vol. 104, no. 22, pp. 221110-221115, June 2014.

[2] N. F. Yu, *et al*., "Light propagation with phase discontinuities: Generalized laws of reflection and refraction," *Science*, vol. 334, pp. 333-337, 2011.

[3] X. Li, S. Y. Xiao, B. G. Cai, Q. He, T. J. Cui, and L. Zhou, "Flat metasurfaces to focus electromagnetic waves in reflection geometry," *Opt. Lett.*, vol. 37, no. 23 pp. 4940-4942, Dec. 2012.

[4] P. Y. Chen, C. Argyropoulos, and A. Alù, "Broadening the cloaking bandwidth with non-foster metasurfaces," *Phys. Rev. Lett.*, vol. 111, no. 23, pp. 233001-233014, Dec. 2013.

[5] A. Yu, F. Yang, A. Z. Elsherbeni, J. Huang, and Y. Kim, "An offset-fed X-band reflectarray antenna using a modified element rotation technique," *IEEE Trans. Antennas Propag.*, vol. 60, no. 3, pp. 1619-1624, Mar. 2012.

[6] H. Li, G. Wang, H. Xu, T. Cai, and J. Liang, "X-band phase-gradient metasurface for high-gain lens antenna application," *IEEE Trans. Antennas Propag.*, vol. 63, no. 11, pp. 5144-5149, Nov. 2015.

[7] X. Wan, Y. B. Li, B. G. Cai, and T. J. Cui, "A broadband transformation optics metasurfaces lens," *Appl. Phys. Lett.*, vol. 105, p. 151604, 2014.

[8] J. B. Pendry, "Negative refraction makes a perfect lens," *Phys. Rev. Lett.*, vol. 85, no. 18, pp. 3966-3969, Oct. 2000.

[9] L. D. Palma, *et al*., "Circularly polarized transmit-array with sequential rotation in ka-band," *IEEE Trans. Antennas Propag.*, vol. 63, no. 11, pp. 5118-5124, Nov. 2015.

[10] T. Cai, *et al*., "Ultra-thin polarization beam splitter using 2-D transmissive phase gradient metasurface," *IEEE Trans. Antennas Propag.*, vol. 63, no. 12, pp. 5629-5636, Dec. 2015.

[11] X. Chen, H. F. Ma, X. Y. Zou, W. X. Jiang, and T. J. Cui, "Three dimensional broadband and high-directivity lens antenna made of metamaterials," *Appl. Phys.*, vol. 110, pp. 0449041-0449048, Aug. 2011.

Jianxun Su received the M.S. degree and the Ph.D. degree in Electromagnetic Field and Microwave Technology from the Communication University of China and Beijing Institute of Technology, Beijing, China, in 2008 and 2011, respectively.

From 2012 to 2014, he was with China Electronics Technology Group Corporation (CETC), where he engaged in phased-array system research. He is currently working as Associate Researcher at School of Information Engineering, Communication University of China and also with the Science and Technology on Electromagnetic Scattering Laboratory. His special research interests include integral equation method, computational electromagnetics, metamaterial, phased-array antenna, radar target characteristics.

Zhi Li received the B.S. degree in Henan University, Henan Province, China, in 2013. From 2015 to now, he is pursuing the M.S. degree of Electromagnetic Field and Microwave Technology at Communication University of China, Beijing, China. His research interests include metamaterials, lens antennas, reflector antennas, microstrip array antennas, etc.

Zhengrui Li received the B.S. degree in Communication and Information System from Beijing Jiaotong University, Beijing, China, in 1984; the M.S. degree in Electrical Engineering from Beijing Broadcast Institute, Beijing, China, in 1987; and the Ph.D. degree in Electrical Engineering from Beijing Jiaotong University, Beijing, China, in 2009.

He is currently a Professor with the Communication University of China, Beijing, China. He studied at Yokohama National University, Yokohama, Japan, from 2004 to 2005. His research interests include the areas of finite-difference time-domain (FDTD) methods, electromagnetic scattering, metamaterials and antennas.

Li is a Senior Member of the Chinese Institute of Electronics.

Yaoqing (Lamar) Yang received his B.S. degree from the Northern Jiaotong University, China, and his M.S. degree from the Beijing Broadcast Institute, China, both in Electrical Engineering. He received his Ph.D. degree in the area of Wireless Communications and Networks from the University of Texas (UT) at Austin. He is now an Associate Professor in the Department of Electrical and Computer Engineering, University of Nebraska-Lincoln (UNL).

His current research interests lie in wireless communications, radio propagations, and statistical signal processing. Yang is a Senior Member of IEEE.